SIMULATING DISTANCE SAMPLING TO ESTIMATE NEST ABUNDANCE ON THE YUKON-KUSKOKWIM DELTA, ALASKA

By

Elaine Gallenberg, B.S.

A project submitted in partial fulfillment of
the requirements for the Degree of

Master of Science
in
Statistics

Department of Mathematics and Statistics
University of Alaska Fairbanks
May 2020

APPROVED

Dr. Ron Barry, Committee Chair
Dr. Margaret Short, Committee Member
Dr. Scott Goddard, Committee Member
Dr. Julie McIntyre, Committee Member
Dr. Leah Berman, Chair
Department of Mathematics & Statistics

ABSTRACT

The U.S. Fish and Wildlife Service currently conducts annual surveys to estimate bird nest abundance on the Yukon-Kuskokwim Delta, Alaska. The current method involves intensive searching on large plots with the goal of finding every nest on the plot. Distance sampling is a well-established transect-based method to estimate density or abundance that accounts for imperfect detection of objects. It relies on estimating the probability of detecting an object given its distance from the transect line, or the detection function. Simulations were done using R to explore whether distance sampling methods on the Yukon-Kuskokwim Delta could produce reliable estimates of nest abundance. Simulations were executed both with geographic strata based on estimated Spectacled Eider (*Somateria fischeri*) nest densities and without stratification. Simulations with stratification where more effort was allotted to high density areas tended to be more precise, but lacked the property of pooling robustness and assumed stratum boundaries would not change over time. Simulations without stratification yielded estimates with relatively low bias and variances comparable to current estimation methods. Distance sampling appears to be a viable option for estimating the abundance of nests on the Yukon-Kuskokwim Delta.

Contents

1 Introduction

Estimating abundance is a common and important aspect of the study and management of wildlife. Since 1985, the United States Fish and Wildlife Service (USFWS) has conducted annual surveys on the Yukon-Kuskokwim Delta (YKD), Alaska (Figure 1) to estimate the total number of nests per species of bird. Of special interest is the number of Spectacled Eider (*Somateria fischeri*) nests as this species is federally listed as threatened under the Endangered Species Act and this annual survey is part of its official recovery and monitoring plan (Federal Register 1993; U.S. Fish and Wildlife Service 1996).

The current technique used for estimation of nest abundance involves nest searching on large plots and aerial surveys. For about two weeks each year from about the end of May to mid-June, intensive nest searching takes place on plots within the core nesting area (716 km^2) (Figure 2). Plot sizes have been variable throughout the years, but for most years (1988-1994 and 1997-2019) they were 32.4 ha (402 m x 805m) (Fischer et al. 2017). Then, using a mark-recapture model created in the 1990s, a correction factor is estimated including covariates like species, habitat, and observer experience (Fischer et al. 2017). The correction factor is used to account for nests that went undetected in plots and the result is an estimate of number of nests per species in the core nesting area. In the greater YKD coastal area (12,832 km^2) (Figures 1,2), aerial transects are flown and used to extrapolate the estimate of nests within the core nesting area to the greater YKD coastal area using ratio sampling methods (Fischer et al. 2017).

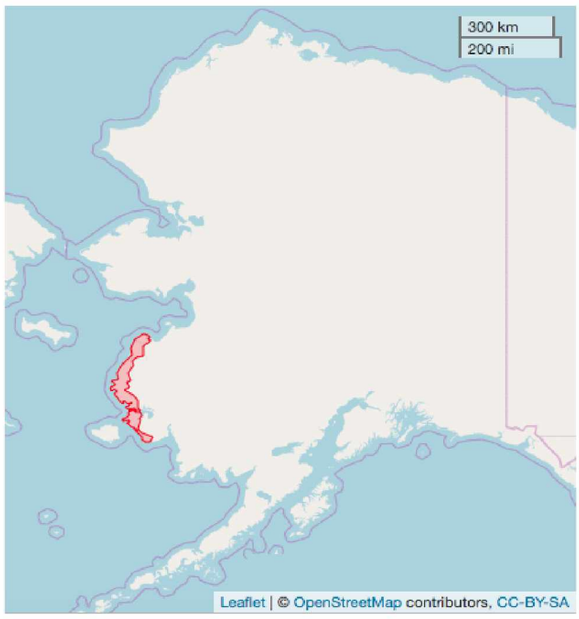

Figure 1. The location of the Yukon-Kuskokwim Delta coastal area within Alaska, USA.

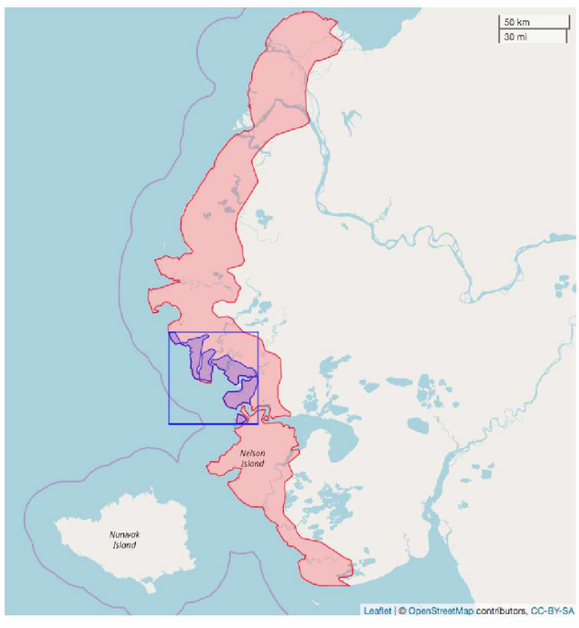

Figure 2. The bounded area (blue) is the core nesting area within the highlighted greater YKD coastal area (red).

Biometrician Erik Osnas of the USFWS office in Anchorage questioned whether distance sampling would be a better method than the one currently used to estimate the abundance of nests on the YKD. Distance sampling is a transect-based method that accounts for objects that go undetected. One reason it is appealing for use on the YKD is because the transect-based searching of distance sampling is potentially more efficient than the plot-based searching of the current method. When walking forward on a transect, observers are always searching new areas as opposed to the current plot searching method where observers end up scanning the same areas multiple times. A more efficient search method could allow more area to be sampled overall in the same amount of time as the current method, which would improve estimates. Another reason the transect-based method seems beneficial is that it is less disturbing to the nesting birds if observers move through their space only once.

The focus of this set of simulations was therefore to explore whether distance sampling on the YKD could give reliable estimates of nest abundance for all species of interest. Special attention was given to trying to make the survey optimal for Spectacled Eider nest detection. Parameters of the simulation were defined using information from the previous USFWS surveys as well as from a small distance sampling pilot study that was done in the 2019 season. The simulation was created and analyzed using the R packages Distance and DSsim which were written and are maintained by some of the creators of and leading experts in distance sampling (R core team 2018, Miller et al. 2019, Marshall 2019).

The objectives of this paper are to explain how the simulation was set up and to explore the results of the simulation along with their implications. The rest of the paper is organized as follows. Section 2 gives an overview of the theory of distance sampling. Section 3 explains why distance sampling seems like a viable way to estimate nest abundance on the YKD and why it may be better than the current method. Section 4 details how parameters for the simulation were chosen and the simulation process. Section 5 shows the results of the simulation and Section 6 is a discussion of these results. After a brief conclusion (Section 7), areas of future research (Section 8) are outlined.

2 Distance Sampling Background and Theory

2.1 Background

Distance sampling is a common and well-understood method to estimate the density or abundance of objects in an area that has been used on a wide variety of taxa from reptiles to birds to marine mammals (Swann et al. 2002, Ruthrauff et al. 2012, Williams and Thomas 2009). Point transects (point counts) and line transects are both forms of distance sampling (Buckland et al. 2001). In line transect distance sampling, observers walk, fly, boat, or drive line transects distributed randomly throughout the study area and record the perpendicular distance of each detected object of interest to the transect line (Swann et al. 2002, , Schmidt et al. 2012, Williams and Thomas 2009, Borralho et al. 1996). Commonly, objects close to or on the line will be detected more often than objects farther from the line. The basis of distance sampling relies on estimating the detection function, which is the probability of detecting an object given its distance from the transect line (Buckland et al. 2001). The detection function is commonly denoted as $g(x)$ where x is is the perpendicular distance from an object to the transect line (Buckland et al. 2001). With enough transects and detections, the detection function can be accurately estimated, which allows for estimation of the density or abundance while accounting for the objects that were present but remained undetected (Greene and Efford 2012).

2.2 Assumptions

There are five critical assumptions (1-5 below) of distance sampling, and two that are less critical (6-7 below), but improve estimation if they are satisfied (Buckland et al 2001). The assumptions are:

1. Transects are distributed randomly throughout the study area.

2. Objects on a transect line are always detected ($g(0) = 1$).

3. Objects are detected at their initial location or are stationary.

4. Perpendicular distances are measured accurately.

5. Objects are identified correctly.

6. Objects near the transect are detected with near certainty. In terms of the detection function, this is called a "shoulder."

7. Detections are independent of one another.

2.3 Theory and Details of Estimation

2.3.1 Conventional Distance Sampling to Estimate Abundance

Line transect sampling can be considered a form of plot sampling where not all objects within a plot are detected. Centered on a transect, the length of a plot is the length of the transect and the width of a plot is $2w$. Usually, w is a defined distance past which detection of an object is very small or impossible, but w can also be infinite (Buckland et al. 2015). Let P_a be the proportion of objects detected in a plot or equivalently, the probability an object is detected given it is within distance w from the line. The estimate of density is then

$$\hat{D} = \frac{n}{2wL\hat{P}_a} \ ,$$

where n is the number of objects detected and L is the sum of the lengths of all transect lines (total effort) (Buckland et al. 2015).

To estimate P_a, the key assumption is that transects were placed independently of object locations or randomly throughout the study area. If this was the case and observers were able to detect every object in each plot, we should expect the distribution of objects with respect to distance from the line to be uniform (Figure 3). If transects were placed randomly, then over many transects there would be no reason to expect more objects at one distance, say 30 m from the transect line, than any other distance.

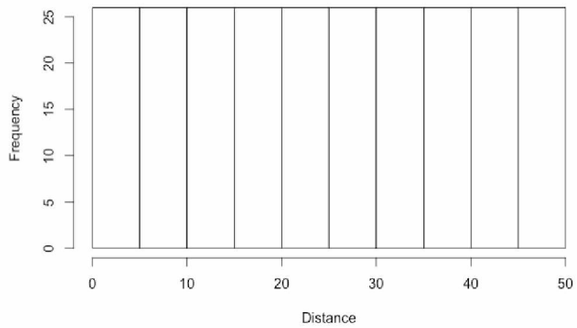

Figure 3. A histogram displaying the expected distribution of objects given distance from the transect line if all objects within w of the line could be detected.

In reality, objects farther from the line are usually harder to detect so in an observed distribution of objects, the frequency of detection declines as distance from the line increases (Figure 4).

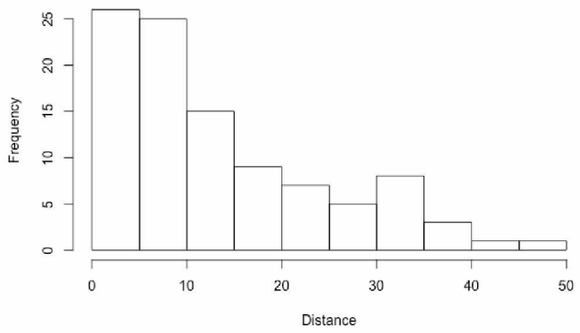

Figure 4. A histogram of what the observed frequencies of detection given distance from the transect may look like with the reality of imperfect detection.

From the observed distance data, the detection function, $g(x)$, can be estimated and scaled to integrate to one so that it is a true probability density function (Figure 5).

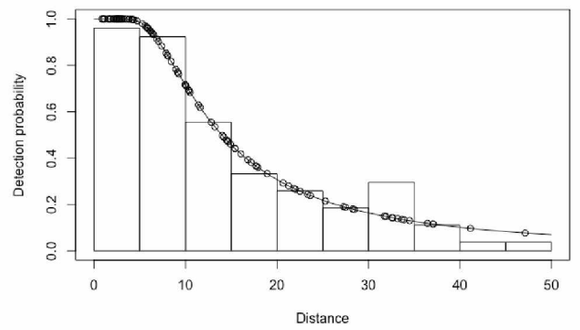

Figure 5. A detection function fitted to the example observations and scaled to be a probability density function. For each detected object, a point was placed on the detection function at its respective perpendicular distance from the transect line.

An estimate of P_a can then be obtained by dividing the area under the curve by the area of the rectangle:

$$\hat{P_a} = \frac{\int_0^w g(x)dx}{(1)w} = \frac{\mu}{w}.$$

In Figure 6, this would be dividing the blue area under the curve (μ) by the total area of the grey rectangle which is just $w(1)$ or in this case $50(1) = 50$.

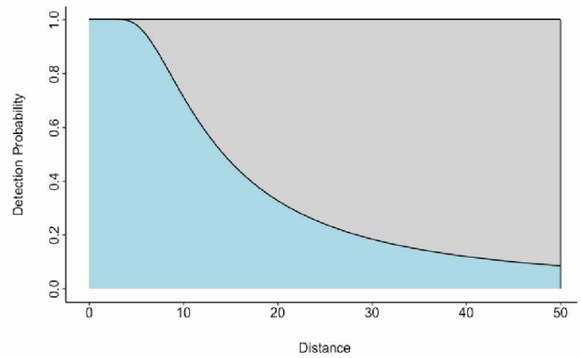

Figure 6. A fitted detection function colored to show the area under the curve, μ, in blue.

Once estimates of P_a and then D are obtained, abundance can be estimated from the simple formula

$$\hat{N} = A\hat{D} = A * \frac{n}{2wL\hat{P_a}} \ ,$$

where A is the area of the study region.

2.3.2 Modelling the Detection Function

To model the detection function used in distance sampling, usually one of three key functions is used. The first is the uniform key function

$$g(x) = \frac{1}{w}, \quad 0 \leq x \leq w$$

which is normally only used if the probability of detection of objects remains very high out to the truncation distance, w. The second is the half-normal function

$$g(x) = exp(-\frac{x^2}{2\sigma^2}), \quad 0 \leq x \leq w$$

and the third, and most flexible, is the hazard-rate function

$$g(x) = 1 - exp[-(\frac{x}{\sigma})^{-b}], \quad 0 \leq x \leq w.$$

Here, σ is a scale parameter and b is a shape parameter (Buckland et al. 2001). The hazard rate function is similar to the cumulative distribution function (CDF) of a Weibull distribution. The difference is the negative exponent in the hazard rate model where there is a positive in the CDF of the Weibull distribution. To allow for greater flexibility, a semiparametric model can be fit by using a cosine series, Hermite polynomial series, or simple polynomials series adjustments with a chosen key function. Estimation of the parameters is done using maximum likelihood methods (Buckland et al. 2001).

2.3.3 Pooling Robustness

In conventional distance sampling, the detection function depends solely on distance from the transect. In reality, there are many factors that may influence detection including observer experience, size of the object, or habitat. Conventional distance sampling relies on a property of the density and abundance estimators called pooling robustness which allows for reliable estimation of density and abundance even when factors that may affect detection are not included in the model (Buckland et al. 2015). To better understand the pooling robustness property, assume that detection depends on observer experience and habitat. For each level or subset of all combinations of observer experience and habitat (inexperienced and habitat A, experienced and habitat B, etc), there would be a corresponding detection curve. An estimate of abundance could be obtained for each subset of the data using its respective detection curve. If an estimate of total abundance was desired, it would be obtained by summing these individuals estimates. A pooled estimate of abundance would pool the data from all subsets, estimate a single detection function without considering observer or habitat, and estimate abundance from that single detection function. The pooled estimator, which does not consider observer or habitat, would be pooling robust if on average, it gave the same estimate as when summing over each subset that did consider observer and habitat (Burnham et al. 1979). When pooling robustness applies, researchers can be confident their estimates are reliable even if not all factors thought to influence detection were included. For more details and a mathematical proof of the pooling robustness property, see Burnham et al. (2004, pp. 389-392).

The estimators used for distance sampling have been shown to have the pooling robustness property in most cases. However, there are situations where the pooling robustness property does not apply. One such situation is if geographic stratification is used and allocation of sampling units to the geographic strata is not proportional to area. Therefore, for five of the seven versions of the simulation performed in this study, the pooling robustness property did not apply. Only the version where allocation was proportional to area of the stratum and the version without geographic strata were pooling robust.

2.3.4 Multiple Covariate Distance Sampling

Even after considering the pooling robustness property, there are cases where the inclusion of covariates that affect detection is needed or desired. If differences in detection due to a covariate are extreme or if estimates for each level of the covariate are desired, then the covariate should be included in the model. For example on the YKD, the detection of nests from Greater White-fronted Goose is easier than the detection of nests from Spectacled Eider and species-specific estimates of nest abundance are desired. Therefore, species should be included as a covariate. When covariates such as this are included to model the detection function, it is called multiple-covariate distance sampling (Buckland et al. 2001).

Instead of pooling observations and using species as a covariate, another option would be to post-

stratify by species and estimate a detection function independently for each species. This would work well if there were an adequate number of detections for each species (60 - 80) (Buckland et al. 2001). However, with species like Spectacled Eider that are less common and more difficult to detect, a high number of observations may be unattainable and estimation of the detection function and abundance would be poor. It may be better then to pool observations and include species as a covariate, as was done in this simulation. The assumption being made when pooling observations is that all species have the same shape in their detection function and vary only due to scale (Buckland et al. 2015). In reality, the decision whether to pool or not could be decided with standard model selection criterion such as AIC.

Another situation where the inclusion of covariates is necessary is if geographic strata are used and allocation of effort to each stratum is not proportional to area. As stated in section 2.3.3, in this case, pooling robustness no longer applies and therefore any factor thought to influence detectability should be modeled (Buckland et al. 2015).

Modelling the detection function changes when covariates are included. The scale parameter, σ, is defined as a function of the covariates such that

$$\sigma(\mathbf{z_i}) = exp(\alpha + \textstyle\sum_{c=1}^{C} \beta_c z_{ic}),$$

where $\mathbf{z_i}$ is a vector with the covariate values for the i^{th} detected object and α, β_1, ..., β_C are coefficients (Buckland et al. 2015). Maximum likelihood methods are used to estimate all parameters and the likelihood is conditioned on the observed covariate values.

2.3.5 Variance of Estimates

The variance of $\hat{D}$ has two components. The first is uncertainty in the estimation of the detection function parameters and by extension, the uncertainty in the estimation of $\hat{P_a}$. The second is from variability in estimating the encounter rate, n/L (Buckalnd et al. 2001). The estimate of the variance of $\hat{D}$ is given by Buckland et al. (2001) as

$$\begin{aligned}\hat{V}(\hat{D}) &= \hat{D}^2 * ([cv(\hat{P_a})]^2 + [cv(\tfrac{n}{L})]^2) \\ &= \hat{D}^2 * ([\tfrac{se(\hat{P_a})}{\hat{P_a}}]^2 + [\tfrac{se(\frac{n}{L})}{\frac{n}{L}}]^2).\end{aligned}$$

The variance of $\hat{N}$ can be estimated with

$$\hat{V}(\hat{N}) = A^2 * \hat{V}(\hat{D}).$$

The estimate of $se(\hat{P_a})$ can be obtained with standard maximum likelihood theory (Buckland et al. 2015). The estimation of the variance of the encounter rate is more complicated. The default in the R packages used for this simulation was an estimator shown by Fewster et al. (2009) to be a robust estimator when sampling units were randomly distributed, as in this simulation. It is

$$\hat{V}(\frac{n}{L}) = \frac{k}{L^2(k-1)} \sum_{i=1}^{k} l_i^2 (\frac{n_i}{l_i} - \frac{n}{L})^2,$$

where l_i is the ith transect or sampling unit, and k is the total number of transects or sampling units.

Another common and robust way to estimate variance that was not used in this simulation is with nonparametric bootstrapping methods (Buckland et al. 2015). The transect lines or sampling units can be resampled with replacement to obtain many estimates of density/abundance that capture the sampling distribution of $\hat{N}$ or $\hat{D}$.

3 Advantages of Distance Sampling on the Yukon-Kuskokwim Delta

Distance sampling is an appealing method for estimating nest abundance on the YKD. First of all, the necessary assumptions of distance sampling (Section 2.2) are satisfied, indicating that distance sampling is an appropriate method. Another reason is that the transect-based method of distance sampling seems potentially more efficient at covering ground and less disturbing to nesting birds than the current plot-based method. In comparison to the current intensive plot search method, distance sampling may be more efficient as observers walking a transect do not cross over themselves and search the same area twice like in the plot search method. This efficiency may allow more area to be surveyed overall, which would improve estimates. Distance sampling may also be less disturbing to the nesting birds than the current method as observers would pass through an area just once.

The current model and method used to estimate the proportion of nests detected in each species is somewhat problematic. In the 1990s, a mark-recapture study was done. Two different teams of observers searched the same plots and the differences in nest detection between the two teams was used to build a model that estimated the probability of detection based on covariates like observer experience, habitat, and species. It has been shown that despite the best fit models including the covariates of plot and year, the model chosen and the one currently used each year is a model that includes neither of those covariates (Erik Osnas, personal communication). Therefore, while there was substantial evidence that detection varied based on year and plot, the model currently used does not account for this. Another issue with the current method is that once an estimate of the proportion of nests detected is obtained from the mark-recapture model, it is treated as a known constant rather than an estimated quantity (Fischer et al., 2017). Because the uncertainty in that estimate is not propagated through to the estimate of abundance, the estimate of the variance of the abundance is biased low. These problems would be avoided with a distance sampling model. With distance sampling, the detection function would be remodeled each year, which would account for the changes in detection due to year that the mark-recapture model showed to be significant. The effect of plot or sampling unit could be explicitly included in the modeling of the detection function or the property of pooling robustness could be relied upon so that estimates would be accurate even if covariates such as sampling unit were not included (see Section 2.3.3). Lastly, with the distance sampling method, the uncertainty in the estimation of the proportion of nests detected would be included in the estimate of the variance of the abundance estimate.

4 Simulating Distance Sampling on the Yukon-Kuskokwim Delta

4.1 Background

I did a simulation to explore whether distance sampling on the YKD could give reliable estimates of nest abundance. The current annual survey is a multi-species survey resulting in nest abundance estimates for each species both in the core nesting area and the greater YKD coastal area. My simulation used four species: Cackling Goose (*Branta hutchinsii*), Greater White-fronted Goose (*Anser albifrons*), Emperor Goose (*Chen canagica*), and Spectacled Eider (*Somateria fischeri*). The simulation resulted in nest abundance estimates for each species in the core nesting area only (not the greater YKD coastal area). Of the seven total different versions of the simulation, all except one used geographic stratification based on estimates of high, medium, and low Spectacled Eider nest density.

4.2 Simulation Set Up

4.2.1 Species

To capture the multi-species aspect of the survey, four species were used in the simulation: Greater White-fronted Goose (GWFG), Cackling Goose (CACG), Emperor Goose (EMGO), and Spectacled Eider (SPEI). I chose these species because they are some of those of greatest interest to researchers and represent a gradient of abundance and detectability. Greater White-fronted Goose and CACG nests are very common on the YKD and are more easily detected than most species' nests. The nests of EMGO are also more detectable, but overall are far less common. The nests of SPEI are somewhat more difficult to detect than the other species and are uncommon (Fisher et al. 2017).

4.2.2 Strata

In some versions of the simulation, to optimize the survey for SPEI nest detection, the study area was divided into regions of estimated high, medium, and low SPEI nest density (Figure 7). The estimates came from a generalized additive model from biometrician Erik Osnas that utilized information from data collected from the current survey method and the R package mgcv (Wood 2017). Six versions of the simulation utilized these geographic strata and one version did not include geographic strata.

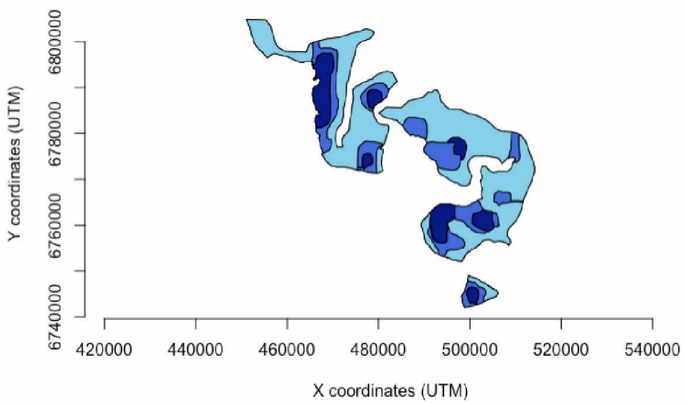

Figure 7. Estimated areas of high (dark blue), medium (blue), and low (light blue) SPEI nest density in the core nesting area of the YKD.

4.2.3 Sampling Unit

Due to the fragmented nature and large area of the YKD core nesting area, the cost of travel is high. Having transects that extend the entire length or width of the region (common in distance sampling survey designs) or even very long transects is unrealistic for foot travel on the YKD as transects would so often be intersected by large sloughs and other bodies of water. Having individual short transects scattered throughout the study area would also be inefficient because so much time would be spent traveling between transects compared to the relatively small amount of time spent actually doing the transect. I therefore made the sampling unit a group of six transects each 1km long divided by 150m (Figure 8). The truncation distance in the simulation was 50m, based on a small pilot study conducted in 2019. The separation of 150m between transects and 50m truncation distance ensured a single nest would not be detected on more than one transect. This setup would allow observers to collect a large amount of information in a single area so that less time would be spent traveling. The simulation treats each sampling unit as if it were one long 6 km transect.

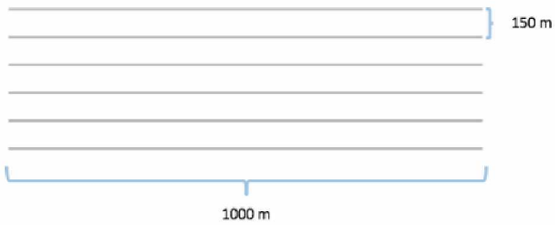

Figure 8. One sampling unit in the simulation was a group of six transects each 1 km long separated by 150 m.

4.2.4 Allocation of Sampling Units

From a small pilot study in 2019, information on the time it would take to complete a transect was gathered. From this I estimated that it would be reasonable for a total of 65-70 sampling units to be completed during the survey's duration (10-14 days). For the six setups that used geographical strata, it was unclear as to how the sampling units should be allocated among the three strata. While there was motivation to allocate additional effort to the high density strata to increase SPEI nest detections, the low density strata covered a large area and therefore could still contain a significant proportion of the total number of nests meaning it should not be neglected. I therefore ran the simulation with six different allocation schemes to try to determine the optimal allocation:

1. 65% Low, 21% Medium, 14% High (Proportional to the area of each stratum)
2. 50% Low, 25% Medium, 25% High
3. 45% Low, 20% Medium, 35% High
4. 40% Low, 30% Medium, 30% High
5. 34% Low, 33% Medium, 33% High
6. 30% Low, 30% Medium, 40% High

For the simulation without geographic strata (standard simple random sampling), the transects and observations from the allocation proportional to area were used, but were analyzed as if there was no geographic stratification.

4.2.5 Detection Function

Based on information from a small pilot study in 2019, the best fit detection function when pooling all species was a hazard rate key function with a scale parameter of 10.278 and shape parameter of 1.994, with standard errors of 2.77 and 0.53 respectively:

$$g(x) = 1 - exp(-(\tfrac{x}{10.278})^{-1.994}),\ 0 \leq x \leq 50.$$

For the simulation, I used two different detection functions: one for SPEI and one for the goose species'. I defined the SPEI nests to be slightly less detectable than average and the goose species' nests to be slightly more detectable than average (Figure 9). This was accomplished by changing the scale parameters to 8.005 and 13.197 for SPEI and the goose species, respectively. The detection function did not vary according to any other covariates such as strata, observer experience, or habitat.

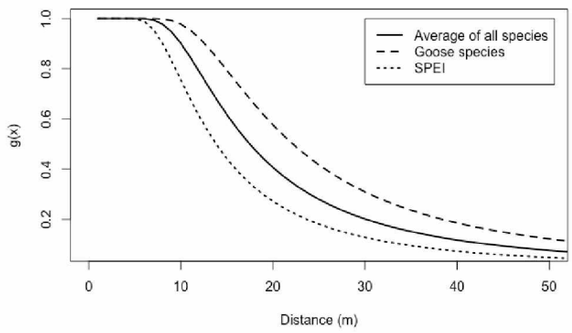

Figure 9. Defined detection function in the simulation for SPEI nests and goose nests compared to the best fit detection function when all species were pooled from the pilot study.

4.2.6 Abundance and Density of Nests

Based on past estimates of the number of each species' nests in the core nesting area, the population size was defined as 96,093 nests with the total number of nests that were CACG, GWFG, EMGO, and SPEI nests being 53,082, 27,175, 11,185, and 4,651 respectively (Fischer et al. 2017). To define the density of the simulated nest population, I used a generalized additive model from biometrician Erik Osnas that estimated the density of nests on the YKD based on all four species in the simulation (Figure 10). I defined the high, medium, and low strata to contain relatively high, medium, and low proportions of SPEI nests, respectively. However, to follow this pattern for all species would be unrealistic because each species exhibits a different distribution of nests and the strata were based on the distribution of SPEI nests only. From individual density maps, I was able to estimate the expected number of each species' nests that would occur in each stratum. I was therefore able to vary the proportion of each species' nests within in each stratum. For example, estimates showed that GWFG nests had a higher proportion in what I called the Low stratum than in the Medium or High strata. Though I could not define density to vary directly due to species, varying the proportion of each species nests in each stratum simulated the heterogeneity of nest density and distribution among species that is actually seen on the YKD.

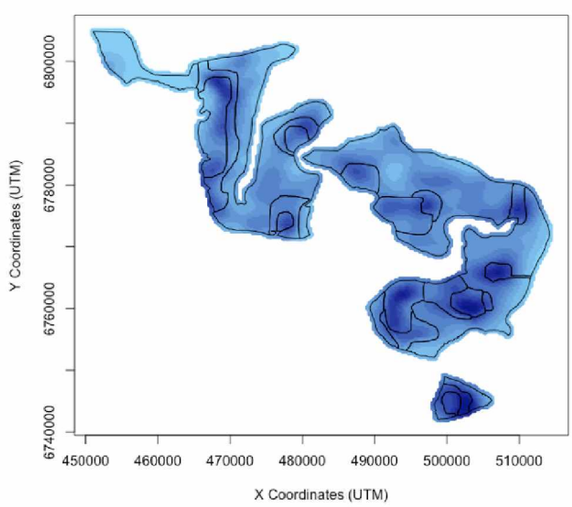

Figure 10. The density map used for the simulations that was based on a generalized additive model with all four species with the strata overlayed.

4.3 Simulation Process

4.3.1 Simulation Packages

This simulation was carried out in a package in R called DSsim and results were analyzed using the package Distance. Both packages were written and are maintained by some of the creators of and leading experts in distance sampling (R core team 2018, Miller et al. 2019, Marshall 2019).

4.3.2 Simulation Steps

A single iteration of the simulations used a population distributed according to the density map, sampling units allocated to the strata according to the desired allocation scheme, and the defined detection function to simulate distance data. A detection function was then fitted to the data and an estimate of abundance was obtained. The steps were as follows:

1. The 96,093 nests were randomly distributed throughout the region according to the provided density map and proportions in each stratum, if applicable (Figure 11).

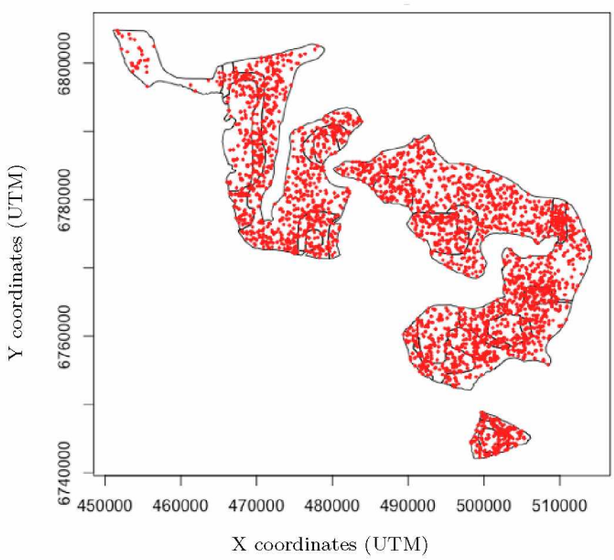

Figure 11. Example random distribution of nests throughout study area according to provided density map.

2. Sampling units were randomly distributed throughout the study area according to the provided allocation scheme (Figure 12).

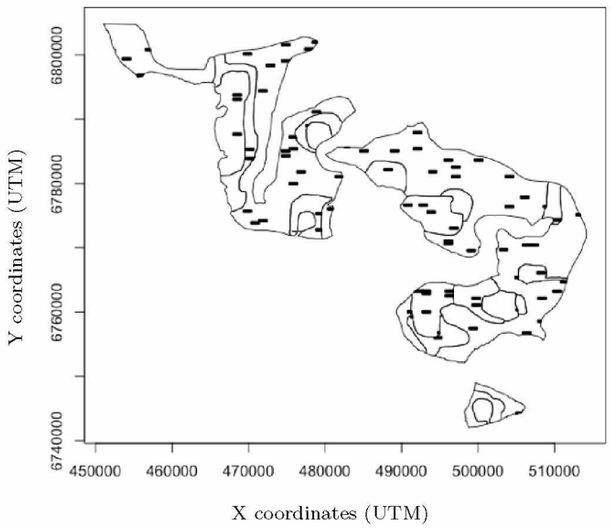

Figure 12. Example random allocation of sampling throughout the study area according to provided allocation scheme.

3. The sampling process was simulated according to the provided detection function. For all nests within the provided maximum distance from the transect line (50 m here), it was determined whether each nest was detected according to the probability of detection from the detection function (Figure 9).

4. The information (species, distance to transect line) from the detected nests in step 3 was stored and simulates what the recorded data would look like if the survey were done in reality.

5. A common detection function pooling all species was fitted to the simulated distances and then a separate scale parameter was estimated for each individual species resulting in species-specific detection functions that relied on pooled data.

6. From the species-specific detection functions, an estimate of P_a was obtained which allowed for estimation of nest abundance for each species.

Steps 1-6 were repeated 120 times for each variation of the simulation (seven variations total).

4.3.3 Use of a High Performance Computer

Because of the large population size (96,093 nests) and fine grid spacing over the study area required to have a population of that size, it took about 28 hours to complete the six steps in a single iteration. Therefore, this work was supported in part by the high-performance computing and data storage resources operated by the Research Computing Systems Group at the University of Alaska Fairbanks Geophysical Institute. Using nodes with 24 cores each, 24 iterations were able to be run at a time per node.

5 Simulation Results

Histograms for the 120 repetitions of each version of the simulation can be found below and summary statistics for each can be found in the appendix.

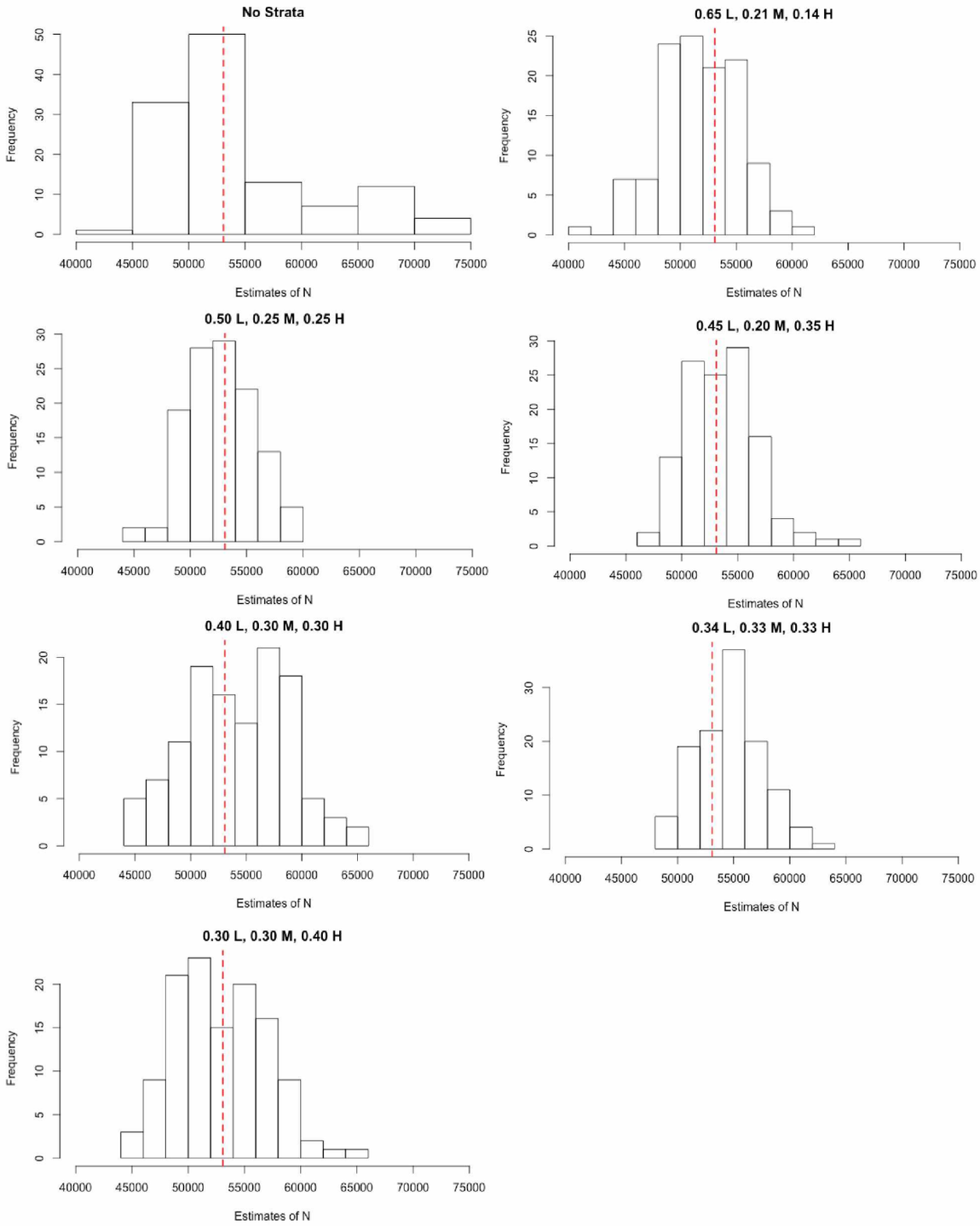

Figure 13. Histograms of the 120 estimates of Cackling Goose nest abundance for each simulation version with the true abundance marked with a red line.

GWFG

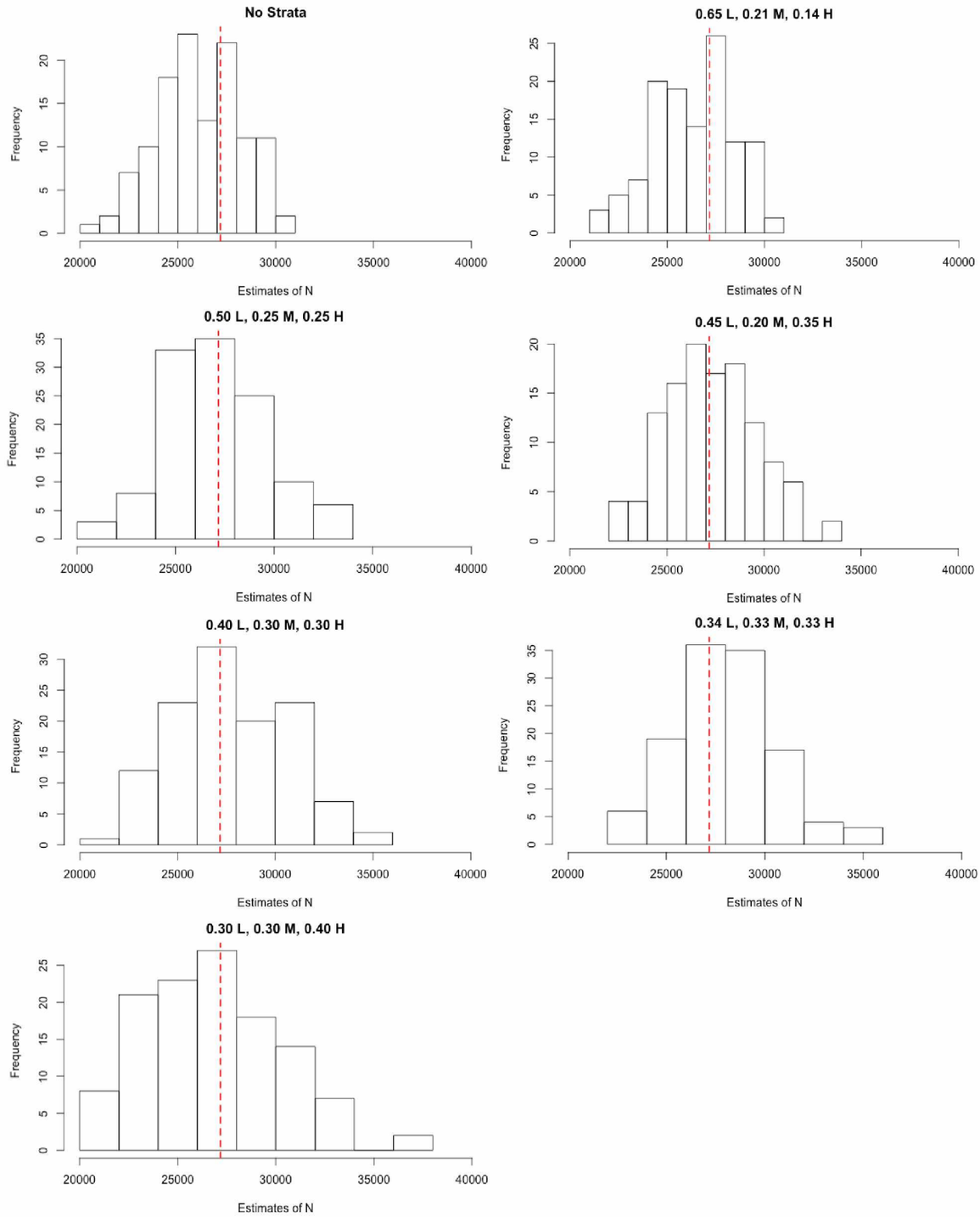

Figure 14. Histograms of the 120 estimates of Greater White-fronted Goose nest abundance for each simulation version with the true abundance marked with a red line.

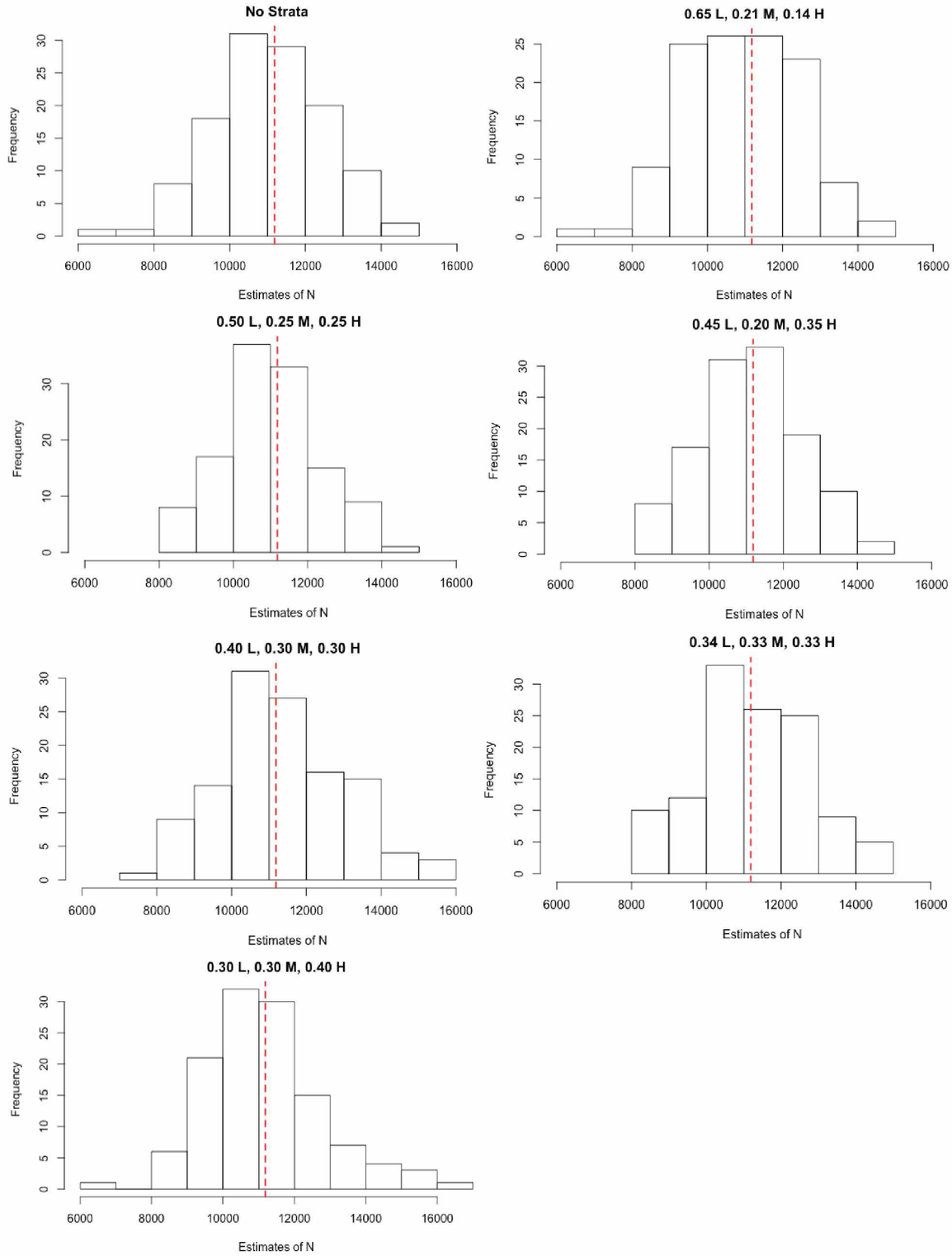

Figure 15. Histograms of the 120 estimates of Emperor Goose nest abundance for each simulation version with the true abundance marked with a red line.

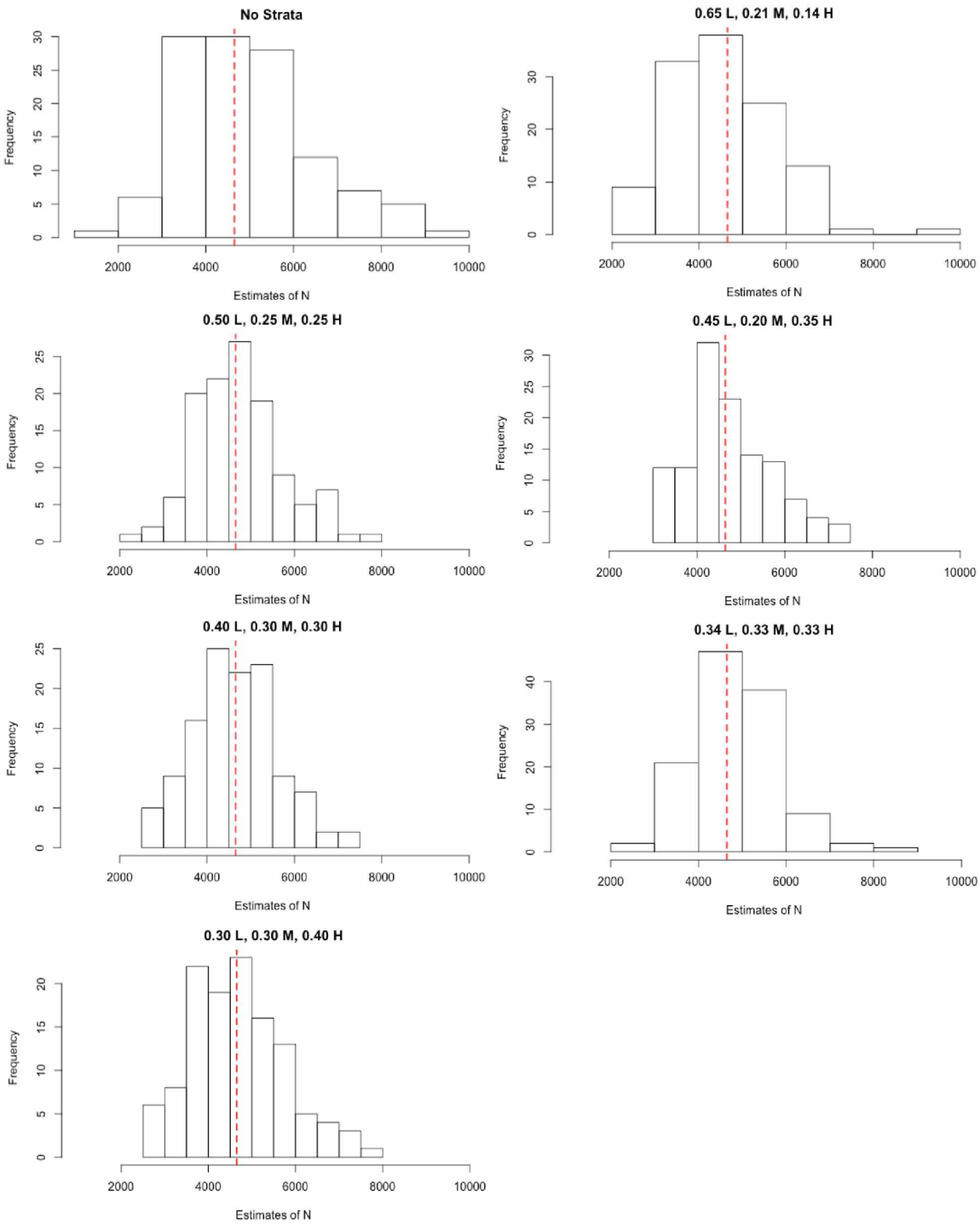

Figure 16. Histograms of the 120 estimates of Spectacled Eider nest abundance for each simulation version with the true abundance marked with a red line.

For CACG nests, all setups resulted in fairly unimodal and symmetric sampling distributions (Figure 13). The simulation without geographic strata deviated from this the most with some estimates falling well above the true value resulting in a slightly right-skewed distribution (Figure 13). All had relatively small bias with the largest estimated as 3.02% from the 35% Low, 33% Medium, 33% High setup (Table 5). The setup without geographical strata had the largest standard deviation (Table 2). The setup with the smallest standard deviation was 50% Low, 25% Medium, 25% High (Table 2). The setup that resulted in the greatest average number of nest detections was the 30% Low, 30% Medium, 40% High setup. In general, nest detections for CACG increased as more effort was allocated to the High stratum (Table 4).

For GWFG nests, again all setups resulted in fairly unimodal and symmetric sampling distributions (Figure 14). The setup with the largest estimated percent bias was the one without geographic strata at -3.91% (Table 5). The setup with the largest standard deviation was the 30% Low, 30% Medium, 40% High

setup and the one with the smallest was 65% Low, 21% Medium, 14% High (Table 2). Average sample size was very similar across all setups except for the 30% Low, 30% Medium, 40% High one, which had fewer average nest detections (Table 4).

The sampling distributions of estimates of the number of EMGO nests were also unimodal and symmetric (Figure 15). The 65% Low, 21% Medium, 14% High had the largest estimated percent bias at -2.20% so all setups had small bias (Table 5). The setup with the largest standard deviation was 40% Low, 30% Medium, 30% High and the setup with the lowest was 50% Low, 25% Medium, 25% High (Table 2). Average sample size was lowest in the setups without geographic strata and proportional to area and highest in the 34% Low, 33% Medium, 33% High setup (Table 4).

Lastly, the sampling distributions of estimates of the number of SPEI nests also displayed fairly unimodal and symmetric shapes, although in general the estimated percent bias for SPEI nests was larger than for other species' nests indicating a greater deviation from being symmetric (Figure 16, Table 5). The setup without geographic strata was slightly right-skewed resulting in the largest estimated percent bias of 6.74% (Table 5). The setup with the largest standard deviation was the one without strata and the one with the smallest was 34% Low, 33% Medium, 33% High (Table 2). As with CACG, nest detections generally increased as more effort was allocated to the High stratum (Table 4).

6 Discussion

Cackling Goose nests were the most abundant in the simulation with 53,082 nests total. The nests were fairly high density across the study area, but more dense in the High and Medium strata than the Low stratum. This is most likely why average nest detection for CACG nests increased as more effort was allocated to the High stratum (Table 4). The standard error of the number of CACG nests in the core nesting area from 2016 with the current sampling method was estimated as 5,502 (Table 2). Note that estimates of standard error from the current method are biased low because estimation of the detection probability was treated as a known value so uncertainty in this estimate was not included in the estimate of N. All simulation setups resulted in standard deviations smaller than this except the simulation without geographic strata which had a standard deviation of 6,689.52 (Table 2).

Greater White-fronted Goose nests were the second most abundant with a total of 27,175. Their density was highest in the Low stratum which most likely explains why in the 30% Low, 30% Medium, 40% High setup nest detections were lowest and standard deviation was highest (Table 4; Table 2). The standard error of the number of GWFG nests in the core nesting area from 2016 with the current sampling method was estimated as 2,360 (Table 2). The setup without geographic strata, 65% Low, 21% Medium, 14% High setup, and 45% Low, 20% Medium, 35% High setup had standard deviations lower than this while the rest were higher. (Table 2)

Emperor Goose nests had the highest density in the Low stratum and lowest density in the High stratum with 11,185 nests total. The standard error of the number of EMGO nests in the core nesting area from 2016 with the current sampling method was estimated as 1,096 (Table 2). Only the setups without strata and allocation proportional to area had standard deviations greater than this (1560.02 and 1190.3 respectively) (Table 2).

Spectacled Eider nests totaled just 4,651 and their density aligned with the High, Medium, and Low stratum. The standard error of the number of SPEI nests in the core nesting area from 2016 with the current sampling method was estimated as 1,094 (Table 2). All setups had standard deviations smaller than this expect the setup without geographic stratification, which had a standard deviation of 1560.02 (Table 2).

Overall, there was not a universally best set up or allocation. Each set up and allocation had its own set of advantages, disadvantages, and properties that should be considered.

In general, when using geographic strata that allocated more effort to areas of high SPEI nest density, detection of SPEI nests was relatively high and precision in general was better compared to when effort

was allocated proportionally to area or when no stratification was used (Table 4, Table 2). However, there are two large disadvantages when using geographical strata and allocation is not proportional to area. The first is that the property of pooling robustness no longer applies (Buckland et al. 2015). This means any covariates that cause differences in detection should be explicitly included in the model. Another is that in the context of long-term monitoring, there is an assumption that strata boundaries remain the same (E. Rexstad, personal communication). This is an unrealistic assumption as the number of SPEI nests on the YKD has displayed an increasing trend since the mid-1990s, which implies the distribution and density of nests will continue to change.

The only setup of the simulation that avoided the disadvantages listed above was the one without geographical stratification, or the approximation of standard simple random sampling. While the estimated standard error of estimates from this setup were higher than when stratification and disproportional allocation were used, the estimates overall had relatively low bias and standard errors comparable, even if slightly higher, to those from the current method (Table 2).

In some aspects, the setup and analysis of the simulation may under represent the amount of bias and variation that could be expected if distance sampling were to be used on the YKD. One way in which it may have underestimated was that the defined true shape of the detection function was the same for all species and only varied by scale (Section 3.2.5). This is what is assumed to be true when pooling observations and using species as a covariate, as in this simulation. In reality, if the shape of the detection function was different for each species, but the analysis was still a pooled analysis, the estimates may not be as reliable because a detection function with the wrong shape would be used for estimation of abundance in some species. Another aspect is the fact that the defined true detection function did not depend on anything except distance and species. When sampling effort is not proportional to geographical strata, pooling robustness no longer applies so if there is heterogeneity in detection due to covariates not included in the model, the estimates may be biased. The defined true detection function did not depend on any factors other than those included in the model so the loss in the pooling robustness property was not tested.

In other aspects, the simulation may have over estimated the amount of bias and variation. One setup that could lower the amount of variation would be to use a systematic sampling design over the random sampling design showed here because variance in encounter rates tends to be lower with systematic designs than completely random designs (Buckland et al. 2001). Another aspect that may lower variance and bias would be to use a smaller truncation distance than 50 m. When fitting the detection function, it is more important to have a good fit at distances near zero than farther distances. In most simulations, there were few detections past 30 m or 40 m from the line. By including all observations out to 50 m when fitting the model, as was done in this simulation, the model may sacrifice a close fit at small distances to accommodate very far distances. This may result in a poorer fitting model and therefore less reliable estimates than if data were truncated.

7 Conclusion

Based on the simulations run for this project, distance sampling seems to be a viable option for reliable estimation of nest abundance on the YKD. If improving the number of SPEI nest detections and increasing precision is a main priority, geographical stratification with more effort allocated high density areas seems to be the best setup. The significant disadvantages of this are a loss of the pooling robustness property and a somewhat unrealistic assumption that stratum boundaries remain unchanged over time. To avoid these disadvantages, a sampling technique without geographic stratification could be employed. The simulation from this setup indicated results would be relatively unbiased with standard deviations larger than setups taking advantage of geographic stratification, but similar to the estimated standard error of the current sampling methods. Further improvements could come from systematically placing the sampling units rather than placing them completely randomly and using a smaller truncation distance when analyzing the data.

8 Future Research

There are many other aspects and versions of this simulation left to be explored. One aspect would be to investigate if and how much different levels of effort improve abundance estimates. A pilot study may be done in June of 2020 on the YKD to improve the estimate of how many sampling units would be possible over the course of the survey. Another version could test the pooling robustness property by defining the detection function to depend on another covariate, such as observer experience, but not include that covariate in the analysis. It would also be beneficial to investigate how much results change if the true detection function has a different shape for each species, but the species are still pooled to estimate a detection function where the same shape is the same.

9 References

Borralho, R., Rego, F., Vaz Pinto, P. 1996. Is driven transect sampling suitable for estimating red-legged partridge Alectoris rufa densities?. Wildlife Biology, 2(3), 259-268. doi: 10.2981/wlb.1996.029.

Buckland, S.T.; Anderson, D.R.; Burnham, K.P.; Laake, J.L.; Borchers, D.L.; Thomas, L. 2001: Introduction to distance sampling: estimating abundance of biological populations. Oxford University Press, Oxford, UK.

Buckland, S.T., Rexstad, E., Marques, T.A, Oedekoven, C.S. 2015. Distance Sampling: Methods and Applications. Springer, Heidelberg.

Burnham, K., Anderson, D., Laake, J. 1979. Robust Estimation from Line Transect Data. The Journal of Wildlife Management, 43(4), 992-996. doi: 10.2307/3808290.

Burnham, K.P., Buckland, S. T., Laake, J. L., Borchers, D. L., Marques, T. A., Bishop, J. R. B., Thomas, L. 2004. Further topics in distance sampling. pp. 307-392 in Buckland, S.T., Anderson, D. R., Burnham, K. P., Laake, J. L., Borchers, D. L., Thomas, L. (Eds.), *Advanced Distance Sampling.* Oxford: Oxford University Press.

Federal Register. 1993. Final rule to list the spectacled eider as threatened. Federal Register 58: 27474-27480.

Fewster, R., Buckland, S., Burnham, K., Borchers, D., Jupp, P., Laake, J., Thomas, L. 2009. Estimating the Encounter Rate Variance in Distance Sampling. Biometrics, 65(1), 225-236. URL www.jstor.org/stable/25502262

Fischer, J. B., Wlliams, A. R., and R. A. Stehn. 2017. Nest population size and potential production of geese and spectacled eiders on the Yukon-Kuskokwim Delta, Alaska, 1985-2016. Unpubl. Rep., U.S. Fish and Wildlife Service, Anchorage, AK.

Greene, T., Efford, M. 2012: Birds: estimates of absolute density and abundance-distance sampling. New Zealand Government. DOCDM-534993.

Laura Marshall. 2019. DSsim: Distance Sampling Simulations. R package version 1.1.4. https://CRAN.R-project.org/package=DSsim.

Miller, D. L., Rexstad, E., Thomas, L., Marshall, L., Laake, J.L. 2019. "Distance Sampling in R." Journal of Statistical Software, 89(1), 1-28. doi: 10.18637/jss.v089.i01 (URL: http://doi.org/10.18637/jss.v089.i01).

R Core Team. 2018. R: A language and environment for statistical computing. R Foundation for Statistical Computing, Vienna, Austria. URL https://www.R-project.org/.

Ruthrauff, D.R.; Tibbitts, T.L.; Gill, R.E.; Dementyev, M.N.; Handel, C.M. 2012: Small population size of the Pribilof rock sandpiper confirmed through distance-sampling surveys in Alaska. The Condor, 114(3), 544-551. doi: 10.1525/cond.2012.110109.

Schmidt, J. H., Rattenbury, K. L., Lawler, J. P., MacCluskie, M. C. 2012. Using distance sampling and hierarchical models to improve estimates of Dall's sheep abundance. Journal of Wildlife Management, 76, 317–327. doi: 10.1002/jwmg.v76.2.

Swann, D.E.; Averill-Murray, R.C.; Schwalbe, C.R. 2002: Distance Sampling for Sonoran Desert Tortoises. The Journal of Wildlife Management, 66(4), 969-975. URL https://www.jstor.org/stable/3802929.

U.S. Fish and Wildlife Service. 1996. Spectacled eider recovery plan. Unpublished USFWS document, Anchorage, AK.

Williams, R. and Thomas, L. 2009. Cost-effective abundance estimation of rare animals: Testing performance of small-boat surveys for killer whales in British Columbia. Biological Conservation, 142(7), 1542-1547.

doi: 10.1016/j.biocon.2008.12.028.

Wood, S.N. 2017. Generalized Additive Models: An Introduction with R (2nd edition). Chapman and Hall/CRC.

10 Appendix

Table 1: Average estimate of nest abundance per setup per species.

Species	No Strata	.65L.21M.14H	.5L.25M.25H	.45L.2M.35H	.4L.3M.3H	.34L.33M.33H	.3L.3M.4H	True
CACG	54367.48	51758.20	52734.95	53580.54	54232.48	54683.30	52868.24	53082
GWFG	26112.60	26313.57	27060.14	27288.41	27708.46	28008.28	26803.96	27175
EMGO	11066.34	10938.66	10999.33	11119.24	11358.17	11248.54	11157.42	11185
SPEI	4964.51	4544.69	4743.58	4763.71	4646.70	4838.85	4665.10	4651

Table 2: Standard deviation of the estimates of nest abundance per setup per species and standard error estimates from the current method in 2016. Note that the standard error estimates from 2016 are biased low.

Species	No Strata	.65L.21M.14H	.5L.25M.25H	.45L.2M.35H	.4L.3M.3H	.34L.33M.33H	.3L.3M.4H	SE of N Est. from current method 2016
CACG	6689.52	3580.94	2949.63	3246.61	4613.53	3063.26	4058.07	5502
GWFG	2197.72	2123.89	2621.55	2331.59	2988.29	2516.36	3437.58	2360
EMGO	1475.79	1486.87	1318.69	1333.06	1657.73	1434.08	1646.23	1096
SPEI	1560.02	1190.30	989.20	981.65	961.98	960.77	1048.12	1094

Table 3: Average CV of the estimates of nest abundance per setup per species where $cv(\hat{N}) = \frac{se(\hat{N})}{\hat{N}}$.

Species	No Strata	.65L.21M.14H	.5L.25M.25H	.45L.2M.35H	.4L.3M.3H	.34L.33M.33H	.3L.3M.4H	CV of N Est. from current method 2016
CACG	0.08	0.07	0.07	0.07	0.07	0.07	0.07	0.10
GWFG	0.09	0.09	0.09	0.09	0.09	0.09	0.1	0.08
EMGO	0.13	0.13	0.13	0.13	0.13	0.13	0.14	0.11
SPEI	0.24	0.23	0.22	0.21	0.21	0.21	0.21	0.18

Table 4: Average sample size (number of nests detected) per setup per species.

Species	No Strata	.65L.21M.14H	.5L.25M.25H	.45L.2M.35H	.4L.3M.3H	.34L.33M.33H	.3L.3M.4H
CACG	844.57	844.57	890.46	996.70	995.08	1049.82	1030.57
GWFG	406.73	406.73	400.81	407.09	409.13	410.89	382.99
EMGO	169.99	169.99	173.12	178.95	182.32	187.35	177.26
SPEI	50.44	50.44	56.43	64.95	63.92	70.46	70.88

Table 5: Estimated percent bias $(\frac{\bar{\hat{N}}-N}{N} * 100)$ per setup per species.

Species	No Strata	.65L.21M.14H	.5L.25M.25H	.45L.2M.35H	.4L.3M.3H	.34L.33M.33H	.3L.3M.4H
CACG	2.42	-2.49	-0.65	0.94	2.17	3.02	-0.40
GWFG	-3.91	-3.17	-0.42	0.42	1.96	3.07	-1.37
EMGO	-1.06	-2.20	-1.66	-0.59	1.55	0.57	-0.25
SPEI	6.74	-2.28	1.99	2.43	-0.09	4.04	0.31